



UNIVERSITY OF LEEDS

This is a repository copy of *Decadal-scale changes of the Ödenwinkelkees, Central Austria, suggest increasing control of topography and evolution towards steady state*.

White Rose Research Online URL for this paper:
<http://eprints.whiterose.ac.uk/85275/>

Version: Accepted Version

Article:

Carrivick, JL, Berry, K, Geilhausen, M et al. (5 more authors) (2015) Decadal-scale changes of the Ödenwinkelkees, Central Austria, suggest increasing control of topography and evolution towards steady state. *Geografiska Annaler, Series A: Physical Geography*, 97 (3). 543 - 562. ISSN 0435-3676

<https://doi.org/10.1111/geoa.12100>

Reuse

Unless indicated otherwise, fulltext items are protected by copyright with all rights reserved. The copyright exception in section 29 of the Copyright, Designs and Patents Act 1988 allows the making of a single copy solely for the purpose of non-commercial research or private study within the limits of fair dealing. The publisher or other rights-holder may allow further reproduction and re-use of this version - refer to the White Rose Research Online record for this item. Where records identify the publisher as the copyright holder, users can verify any specific terms of use on the publisher's website.

Takedown

If you consider content in White Rose Research Online to be in breach of UK law, please notify us by emailing eprints@whiterose.ac.uk including the URL of the record and the reason for the withdrawal request.



eprints@whiterose.ac.uk
<https://eprints.whiterose.ac.uk/>

Decadal-scale changes of the Ödenwinkelkees, central Austria, suggest increasing control of topography and evolution towards steady state

Jonathan L. Carrivick^{1*}, Katie Berry¹, Martin Geilhausen², William H. M. James¹, Christopher Williams³, Lee E. Brown¹, David M. Rippin⁴, Steve J. Carver¹

¹School of Geography, University of Leeds, Woodhouse Lane, Leeds, West Yorkshire, LS2 9JT. UK.

²Department of Geography and Geology, University of Salzburg, Hellbrunnerstrasse 34, A-5020 Salzburg, Austria

³Bristol Glaciology Centre, School of Geographical Sciences, University of Bristol, University Road, Bristol, BS8 1SS. UK.

⁴Environment Department, University of York, Heslington, York, YO10 5DD. UK.

*Correspondence to:
Dr. Jonathan Carrivick,
Email: j.l.carrivick@leeds.ac.uk
Tel.: 0113 343 3324

Abstract

Small mountain glaciers have short mass balance response times to climate change and are consequently very important for short-term contributions to sea level. However, a distinct research and knowledge gap exists between (i) wider regional studies that produce overview patterns and trends in glacier changes, and (ii) in situ local scale studies that emphasise spatial heterogeneity and complexity in glacier responses to climate. This study of a small glacier in central Austria presents a spatiotemporally detailed analysis of changes in glacier geometry and changes in glaciological behaviour. It integrates geomorphological surveys, historical maps, aerial photographs, airborne LiDAR data, ground-based dGPS surveys and Ground Penetrating Radar surveys to produce 3D glacier geometry at thirteen time increments spanning from 1850 to 2013. Glacier length, area and volume parameters all generally showed reductions with time. The glacier equilibrium line altitude increased by 90 m between 1850 and 2008. Calculations of the mean bed shear stress rapidly approaching less than 100 kPa, of the volume-area ratio fast approaching 1.458, and comparison of the geometric reconstructions with a 1D theoretical model could together be interpreted to suggest evolution of the glacier geometry towards steady state. If the present linear trend in declining ice volume continues, then the Ödenwinkelkees will disappear by the year 2040, but we conceptualise that non-linear effects of bed overdeepenings on ice dynamics, of supraglacial debris cover on the surface energy balance, and of local topographically-driven controls; namely wind-redistributed snow deposition, avalanching and solar shading, will become proportionally more important factors in the glacier net balance.

Keywords: mountain glacier; glacier geometry; response time; ELA; LiDAR

40 **Introduction**

41 Small mountain glaciers are extremely important indicators of climate change due to their
42 fast response times (Raper and Braithwaite, 2006; Dyurgerov and Meier, 2000; Haeberli et
43 al., 2007). On a global scale small mountain glaciers (i) are so numerous that they have a
44 significant contribution to the world's total ice volume and may be a notable source of error if
45 excluded (Bahr and Radic, 2012) and, (ii) are much more important for short term
46 contributions to sea level than that from Greenland or Antarctica (Raper and Braithwaite,
47 2006; Glasser et al., 2011). On a local scale, mountain glacier ice mass variations and the
48 consequent changes in meltwater runoff magnitude and timing is of concern for
49 understanding proglacial geomorphology and sediment fluxes (e.g. Carrivick et al., 2013;
50 Carrivick and Rushmer, 2009) and riparian ecology, and in application for power generation,
51 irrigation, and tourism.

52

53 Understanding small mountain glacier mass balance, especially processes representing
54 responses to climate, is most ideally achieved with local direct measurements; i.e. distributed
55 surface elevation and ice and snow density measurement programs. Such field studies are (i)
56 limited to a few tens of points at most on a glacier surface so require extrapolation to the
57 whole glacier, (ii) are expensive in time and resources required and (iii) are consequently
58 rare; in the European Alps there are ~ 25 glaciers now with these programs (Vincent et al.,
59 2004; Zemp et al., 2008). Furthermore, direct mass balance measurements were not initiated
60 until late 1940s and many of these records are intermittent.

61

62 Given the deficiencies in the coverage of direct mass balance data, there have therefore been
63 a series of efforts to analyse changes in glacier terminus position, which are often reported as
64 glacier length changes (in the European Alps; e.g. Hoelzle et al., 2003; Klok and Oerlemans,
65 2004; Oerlemans, 2005; Hormes et al., 2006; Zemp et al., 2008). Indeed Zemp et al. (2008)
66 report on over 200 European Alps glaciers with > 18 terminus position measurements since
67 1850. However, prior to 1890 there were only ~10 European glaciers with measured terminus
68 positions. Furthermore, there is a strong bias towards larger glaciers in the length
69 measurement sample due to the remote location of most small glaciers. Perhaps most
70 crucially, whilst glacier length records can correlate well with weather patterns, albeit with a
71 lag time (or 'response time'), dynamic reactions of a glacier to climate change must be
72 assessed with consideration of area and volume (Harrison et al., 2009 in Paul, 2010).

73

74 Analyses of changes in glacier area and ice surface elevation have relied on (i) field-based
75 geomorphological surveys of moraine crests and contemporaneous ice limits, (ii) remote
76 sensing; either photogrammetry for local-scale studies or image-processing of satellite data,
77 for regional studies (Paul et al., 2002, 2007a; Paul and Haeberli, 2008), the latter which
78 restricts studies to the 1970s onwards, or (iii) climate-driven ice dynamics models. One of the
79 simpler remote sensing approaches is that of the repeated observations of glacier transient
80 snow lines (Chinn, 1995), which at the end of the summer can approximate the ELA, and
81 which can permit high resolution spatiotemporal analyses (e.g. Carrivick and Chase, 2011).
82 Perhaps the ultimate expression of the remote sensing approach is represented by glacier
83 inventories, such as the Austrian glacier inventories of 1969 (Gross, 1987) and 1998
84 (Lambrecht and Kuhn, 2007) and the recently revisited French glacier inventories (Gardent et
85 al., 2014), for example. Whilst these inventory-based studies provide insight into spatial
86 variability in glacier changes, they usually consider changes in glacier surface elevation
87 between just two points in time (e.g. Kääb et al. 2002; Paul et al. 2007a; Hoezlze et al. 2007;
88 Lambrecht and Kuhn, 2007) or for glaciers aggregated regionally (e.g. Paul, 2002; Stocker-
89 Waldhuber et al., 2012).

90
91 There is therefore a lack of consideration of decadal-scale changes at individual glaciers, and
92 a lack of information on absolute volume, which necessitates knowledge of ice thickness and
93 bed topography (Paul et al, 2007b). Knowledge of ice thickness and hence of bed elevation
94 are necessary not only for computing absolute changes in glacier volume, which is of
95 necessity when projecting glaciological changes into the future (c.f. Huss, 2012), but also for
96 determining ice flow mechanics, which is a crucial step in understanding processes that could
97 explain reconstructed geometric changes; see the critical review on previous ice dynamics
98 reconstructions by Carr and Colman (2007). However, the complexity of obtaining direct data
99 in the field on ice thickness and bed elevation, most usually from Ground Penetrating Radar
100 (GPR), means that even then considerable uncertainty can be inherent in the data and
101 interpolation between survey lines is necessary (e.g. Binder et al., 2009). Thus studies of
102 volume changes in mountain glaciers usually report relative volume changes (e.g. Bauder et
103 al., 2007; Villa et al., 2007; Stocker-Waldhuber et al., 2012) without any knowledge of
104 distributed ice thickness and hence of absolute volume. Indirect approaches to estimating
105 absolute volume have been developed; namely (i) relatively simple volume-area scaling
106 (Bahr et al., 1997), (ii) reconstructions using moraine crests, (iii) flow line ‘perfect-plasticity’
107 models (e.g. Li et al., 2012), and (iv) more complex physics-based models (e.g. Farinotti et

108 al., 2009). Climate-driven ice-dynamics models that reconstruct ice volume are limited to
109 very discrete periods of time, usually the Last Glacial Maximum (LGM) and the Little Ice
110 Age (LIA), where geological evidence in the form of moraine ridges and trimlines can test
111 the model (e.g. Golledge et al., 2012; Harrison et al., 2014).

112
113 Overall, whilst a few hybrid studies exist that have integrated multiple types of data (i.e.
114 remote sensing data with mass balance data; e.g. Haeberli et al., 2007; Abermann et al.,
115 2009), a distinct research and knowledge gap exists between (i) wider regional studies that
116 emphasise spatial heterogeneity and complexity in glacier responses to climate and (ii) in situ
117 local scale studies that develop process-understanding. Therefore, as Haeberli et al. (2007)
118 and Linsbauer et al. (2012) both comment, there is a need for spatio-temporally detailed
119 studies on individual glaciers. In order to achieve spatiotemporally detailed studies, it is
120 possible to augment remote sensing and mass balance data with primary geomorphological
121 surveys and compilation of secondary datasets such as historical maps and historical oblique
122 field sketches. Use of historical maps for glacier reconstructions is exemplified by Hall et al.
123 (2003), Villa et al. (2007), Zumbühl et al. (2008), and Knoll et al. (2009), for example. Use
124 of historical oblique photographs and sketches was made by Steiner (2001) using mono-
125 plotting for georeferencing to reconstruct the Rhone glacier from 1874 onwards.

126
127 The aim of this study is to create a spatiotemporally detailed analysis of changes in glacier
128 geometry and to infer what these mean for glaciological behaviour. This study from the
129 Glockner region in central Austria achieves this aim by integrating geomorphological
130 surveys, historical maps, aerial photographs, airborne LiDAR (ALS) data gridded at 1 m
131 resolution, ground-based dGPS surveys and Ground Penetrating Radar surveys to derive the
132 glacier bed elevation and hence ice-thickness. Altogether these datasets produce
133 measurements of three-dimensional glacier geometry at thirteen time increments spanning
134 from 1850 to 2013. Whilst acknowledging the inherent uncertainty in these data sets, this
135 study contributes to the very small number of studies achieving this spatiotemporal resolution
136 of study of glacier changes.

137 138 **Study area**

139 The Ödenwinkelkees glacier (~47°7'00" 12°30'00"E) is located within the Glockner
140 mountain range within the Hohe Tauern National Park in the Salzburg province of central
141 Austria (**Figure 1**). The Ödenwinkelkees was chosen for this study for four main reasons: (i)

142 availability of (analogue) historical data pertaining to the glacier configuration at high spatial
143 and temporal resolution (**Table 1**), (ii) long term monitoring of the terminus position of the
144 Ödenwinkelkees providing dated moraine ridges (Slupetzky and Teufl, 1991), (iii)
145 availability of airborne LiDAR (ALS) data (Carrivick et al., 2013) which provided excellent
146 positional information for georeferencing the analogue data, (iv) two GPR surveys that
147 together provided reasonable spatial coverage and from which an estimate of ice thickness
148 and bed elevation could be made to derive absolute glacier volumes (**Table 1**). Access to the
149 area is most convenient via the Rudolfshuette, which is the ex-Austrian Alpine Club
150 headquarters, a site of continuous weather and snow monitoring by ZAMG (Austrian
151 Meteorological Institute) and ÖBB (national train company) portal, and is now a mountain
152 hotel.

153
154 Regional climate records for the Alps are available from the ‘HISTALP’ database (ZAMG,
155 2014). HISTALP data aggregates multiple weather station records and those from the NE
156 region, which covers the Odenwinkelkees, show no change in precipitation and ~ 1 °C air
157 temperature increase between 1760 and 2008. Local weather data from the Rudolfshuette
158 was obtained as monthly means, but it only covered the 1960s and 1970s, and comparison of
159 this local dataset with the regional HISTALP means yielded very poor correlation in air
160 temperature and no correlation in precipitation.

161

162 **Georeferencing**

163 All analogue historical maps (**Table 1**) and aerial photographs were georeferenced to the
164 airborne LiDAR (ALS) data as projected in the Universal Transverse Mercator World
165 Geodetic System (UTM WGS 1984 33N) and gridded at 1.0 m resolution, using a spline fit
166 between identifiable points on the terrain that were assumed to be static; such as the Weizsee
167 dams, buildings, roads, major gully heads and major stream confluences (c.f. Mennis and
168 Fountain, 2001). All modern maps were georeferenced using their gridline intersections.
169 Maintaining minimal distortion of the available maps required as wide a point coverage as
170 possible, and some maps were at insufficient resolution or with insufficient geospatial
171 reference to be georeferenced with any confidence so they were discarded from the
172 quantitative analysis of this study; although they were still useful for gaining contextual
173 knowledge of the glacier changes.

174

175 Horizontal errors in georeferencing analogue maps by different authors and aerial
176 photographs are discussed at length by Hall et al. (2003) and Knoll et al., (2009) for example
177 and in **Table 2**, but nonetheless remained extremely difficult to quantify absolutely in this
178 study due to the restriction in georeferencing point pair synthesis, which is a product of both
179 limited identifiable features from topographic maps and disagreements between maps as a
180 function of varying resolution (see **Table 2**). We only used thirteen datasets (of all those
181 listed in Table 1) to limit this study to using those datasets in which we had confidence in the
182 georeferencing. Images of these georeferenced maps are available in the supplementary
183 information. Overall error in reconstructed glacier length and area is reckoned to be $\pm 5\%$, in
184 elevation ± 10 m and in thickness ± 20 m (**Table 2**).

185

186 **Reconstruction of glacier character**

187 **Ice extent and 3D ice surface elevation**

188 The 1850 (last Holocene maximum; Little Ice Age) and 1890 moraine ridges were digitised
189 from the maps by Slupetzky and Teufl (1991) and together with their associated trimlines are
190 very visible in the ALS-derived 2008 DEM (**Fig. 1**) in aerial photographs and on the ground
191 (**Fig. 2a and 2b**). Glacier outlines and contour lines for 1969 and 1998 were obtained in
192 digital format and are from Lambrecht and Kuhn (2007). All other glacier outlines and ice
193 surface contours were manually digitised on screen from each georeferenced topographic
194 map (**Table 1; Fig. 3**), as by Linsbauer et al., (2012) and Paul (2010), for example. Ice
195 surface contours had to be estimated for the 1850 and 1890 datasets and this was achieved in
196 the following steps: (i) the glacier extent polyline was converted to points and elevation data
197 attributed to it using the intersection of it with the 2008 DEM, (ii) contours (polylines) were
198 drawn manually across the surface of the glacier extent to link points with identical elevation
199 at ~ 20 m intervals, but this was not a straight line and the simplest way to estimate the
200 palaeo-surface geometry was to (iii) match the planform curve of this contour to that of the
201 1929 dataset, which in the accumulation zone was concave and in the ablation zone was
202 convex. There is unquantifiable error in the published topographic map ice surface elevation
203 contours, and our reconstruction of the 1850 and 1890 ice surfaces is the most simple (and
204 thus defensible) approach (**Table 2**). Nonetheless, this approach to reconstructing ice surfaces
205 from lateral moraine crests has been used elsewhere, by Carrivick et al., (2012), for example.
206 Furthermore, we note that Paul (2010) has shown that an accurate reconstruction of glacier
207 (outline) extent (area) is much more important than that of the surface elevation for
208 determination of former glacier mass balance. Interpolation between the ice surface contour

209 lines using the ArcGIS ‘Topo to Raster’ (ANUDEM algorithm) tool converted the 20 m ice
210 surface contour lines to a smooth surface. Finally, this reconstructed ice surface was clipped
211 to the glacier outline (**Fig. 3**).

212

213 **Ice thickness and 3D geometry**

214 The area and length of each reconstructed glacier extent was calculated from the digitised
215 glacier outlines. Ice surface long profiles were generated along the same centreline for each
216 time period to ensure comparability between each ice surface. The same centreline was used
217 when measuring the long profile of the bed surface to calculate ice thickness of each
218 reconstructed glacier. Ice thickness data is crucial to gain a better understanding of how
219 climate perturbs glacier changes, but is unknown for most glaciers.

220

221 The Ödenwinkelkees bed elevation was estimated primarily using ground penetrating radar
222 (GPR) data gathered in 1998 by Span et al, (2005) and supplemented by our GPR surveys in
223 2010 (**Fig. 1**). Our April 2010 GPR surveys (**Fig. 2c**) covered a total of 2050 m horizontally
224 and utilised a PulseEkko Pro system, following the protocol used by Rippin et al., (2011). In
225 brief, GPR data were collected while moving continuously; the sledge was hauled manually
226 (**Fig. 2c**), and at a centre frequency of 50 MHz. To accurately locate the GPR on the glacier,
227 real-time kinematic (RTK) differential global positioning (dGPS) system data were
228 simultaneously collected via a Leica GPS500. The rover unit was mounted on the sledge,
229 whilst the base station was located at the Hinterer Schafbichl [47°08'04.21827" N and
230 12°37'41.73905" E, 2352 m a.s.l.] (**Fig. 1**) as positioned accurately (+/- 0.01 m) relative to
231 Salzburg using a 8 hour static occupation of that point. A mean 3D positional accuracy of 0.2
232 m was achieved with the rover in this RTK mode. The GPR data was processed in the
233 software packages ReflexW; filtered to remove low-frequency noise, resampled to a uniform
234 0.5 m step-size as recommended for 50 MHz antennas, migrated using an FK algorithm,
235 bandpass filtered with a pass 30-80 MHz, topographically corrected using the dGPS data,
236 conversion of two-way travel time to ice thickness assuming a radar wave velocity of 0.168
237 m ns^{-1} (cf. Rippin et al., 2011).

238

239 Abermann et al., (2009) discuss in detail the errors associated with GPR data, and our 2010
240 data was no different (**Table 2**). Our processed radargrams were tested for internal
241 consistency by checking the surface and bed elevations at crossover points between
242 intersecting GPR lines. Surface elevation crossover errors were very small with a mean error

243 magnitude of just ± 0.2 m. Bed crossover errors had a mean magnitude of ± 6.7 m, but due to
244 there just being 3 cross-over points (**Fig. 1**) we consider (GPR-derived) bed elevation
245 uncertainty to be ± 10 m. Both the 1998 and the 2010 GPR-derived bed elevation were
246 acquired on a series of transects and along a long profile (**Fig. 1**) and in this study that data
247 was digitised; to georeferenced 3D points, and interpolated using the ArcGIS ‘Topo to
248 Raster’ (ANUDEM algorithm) tool (c.f. Hutchinson, 1989; Abermann et al., 2009; Linsbauer
249 et al, 2012). We acknowledge that given the spacing between the GPR survey transects due to
250 steep ice, crevasses and rock falls, the necessary interpolation leads to an over simplification
251 of reality, which can be crude (Linsbauer et al, 2012). Therefore, the uncertainty in
252 reconstructed ice thickness is ± 20 m; i.e. approaching 50 % in the steep headwall area. An
253 ‘ice-free DEM’ was created by merging the GPR-derived bed elevation for the present glacier
254 extent with elevation data on the rest of the catchment from the 2008 DEM.

255
256 Ice thickness at each historical time interval was estimated by subtracting the ice-free DEM
257 from the respective reconstructed ice surface. Volume of each reconstructed glacier was
258 calculated using the ArcGIS ‘cut and fill’ tool, and 3D elevation changes between successive
259 reconstructed glaciers were calculated using the ArcGIS ‘raster calculator’ tool. We had no
260 choice but to assume that the contemporary valley floor as represented in the 2008 ALS data
261 is the elevation as the bed beneath the reconstructed glacier; i.e. that there has been no valley
262 in-fill (sedimentation), because we do not know the thickness of the Eisboden valley floor
263 sediments. Whilst this thickness of sediments is likely to be at least an order of magnitude
264 less than the reconstructed ice thickness, it must be considered that our reconstructed volumes
265 are a minimum estimate. ArcGIS tool ‘zonal statistics’ produced information on mean,
266 maximum and minimum ice surface elevation and ice thickness at each time interval.
267 Spatially distributed rates of change in ice surface elevation and ice thickness were obtained
268 for each time period by dividing the differenced surface (a DEM of difference: ‘DoD’) by the
269 number of years within the time period.

270
271 To bring this study up to date, a survey of the glacier terminus position and ice surface
272 elevation was conducted in July 2013; the latter comprising a long profile and 6 transects
273 recorded using a Leica GPS500 differential GPS. The dGPS was used in Real Time
274 Kinematic (RTK) mode as described above for the GPR surveys. Interpolation between the
275 dGPS points on glacier terminus, on the long profile and along transects was carried out to
276 produce an ice surface DEM, using the “Topo to raster” tool in ArcGIS. This 2013 survey

277 and hence any subsequent analysis using the 2013 dataset were limited to the lower part of
278 the glacier only due to accessibility.

279

280 **Reconstruction of glacier behaviour**

281 The utility of generating three-dimensional glacier geometries for successive time periods is
282 that it permits quantitative assessment of the physical response of a glacier to climate change.
283 Several key glaciological parameters that are largely dependent on ice geometry were
284 analysed in this study; namely the conceptual parameter of glacier equilibrium line altitude
285 (ELA), and the physical parameters of basal shear stress and theoretical ice surface velocity.
286 A consideration of whether basal sliding and subsole deformation were likely was also made.

287

288 **ELA**

289 The ELA provides a good indicator of glacier response to climate change, acting as a climate
290 proxy both for the past and future glacier extents (Bate, 2008). In this study the ELA was
291 reconstructed for the Ödenwinkelkees for each time period using a number of (map based)
292 methods, thereby recognising that each of these methods has strengths and weaknesses (Benn
293 and Lehmkuhl, 2000; Leonard and Fountain, 2003; Porter, 2001). Therefore, an ELA
294 sensitivity analysis was carried out by comparing the resultant ELA values of five of the most
295 frequently used methods; namely the The Area_x Altitude Balance Ratio (AABR),
296 Accumulation Area Ratio (AAR), glacier Terminus-to-Headwall Altitude Ratio (THAR),
297 Median elevation (H_{med}), and contour inflection (kinematic ELA).

298

299 The AABR firstly weights the mass balance according to the distance above or below the
300 ELA of that area. Secondly, the calculation is refined by considering different linear slopes of
301 the mass balance/altitude curve above and below the ELA. Since many glaciers conform
302 roughly to this specification (Osmaston, 2005), the AABR method-derived ELA serves as a
303 useful first approximation for former glaciers, such as that analysed herein, for which there is
304 no a priori knowledge about their mass balance. We used the freely-available AABR
305 spreadsheet of Osmaston (2005) and simply entered in the contour interval, contour values
306 and area of the glacier for each interval. We then applied balance ratios of 0.5 to 4, at 0.5
307 increments and noted the ELA for each. Osmaston (2005) suggests with his Table 4 to select
308 the ELA with the lowest standard deviation as calculated with different BRs for different
309 glaciers in a region. However, because we are only considering a single glacier we simply
310 calculated the mean.

311

312 The AAR method uses the ratio of the accumulation area to the total glacier area (Carrivick
313 and Brewer, 2004; Bate, 2008) to estimate the ELA. AAR values used in the literature are
314 normally within the region of 0.5 to 0.8; representing steady state conditions (Bate, 2008;
315 Carrivick and Brewer, 2004). In this study it was assumed that the accumulation area
316 accounted for 50 % of the total glacier area. The area between 100 m interval contours was
317 calculated automatically and fed into the equation:

$$318 \quad ELA = \frac{\sum A_i h_i}{\sum A_i}$$

319 where A_i is the area between each 100 m contour interval and h_i is the mid-point altitude for
320 each contour interval. This method includes the error associated with reconstruction of
321 glacier extent and contours (**Table 2**). However, this error is usually quite minor and indeed
322 unavoidable when using historic map data (Bate, 2008).

323

324 The THAR method uses a ratio between the maximum and minimum ice altitude to estimate
325 the ELA. This method cannot consider ice surface geometry. Examples throughout the
326 literature of a THAR ratio have consistently used a ratio of 0.35 to 0.4 for valley and cirque
327 glaciers (Carrivick and Brewer, 2004; Bate, 2008). Therefore this study used the equation:

$$328 \quad ELA = A_t + THAR (A_h - A_t)$$

329 where THAR is a set ratio of 0.4, A_h is maximum altitude (headwall crest altitude) and A_t is
330 the minimum altitude (terminus altitude). Error is introduced when finding maximum and
331 minimum altitudes of a glacier, as these altitudes depend on DEM grid resolution as well as
332 vertical accuracy. In this study, altitudes were automatically identified across the margins of
333 the headwall and along the terminus enabling a mean headwall crest elevation and a mean
334 terminus elevation to be calculated.

335

336 The Hmed method simply uses the median altitude between the headwall and the terminus to
337 estimate the ELA. Its advantages are in its simplicity and speed of calculation (Bate, 2008).

338 The literature suggests that the Hmed method tends to overestimate the ELA, and it must be
339 noted that it does not take into account valley topography, which has a strong control over the
340 distribution of glacier area (Nesje, 1992; Porter, 2001; Carrivick and Brewer, 2004). The
341 Hmed method uses the following equation:

$$342 \quad ELA = (A_h - A_t)/2 + A_t$$

343 where A_h is maximum altitude (headwall crest altitude) and A_t is the minimum altitude
344 (terminus altitude).

345
346 The contour inflection (kinematic ELA) method determines ELA via analysis of the shape of
347 ice surface contours, which tend to change from concave to convex down the glacier profile
348 and thus in the transitional zone (around the ELA) appear relatively flat (Leonard and
349 Fountain, 2003). The contour inflection (kinematic ELA) method is simple conceptually and
350 indeed is based on glaciological physics principles. However, error can be introduced due to
351 ELA estimations when applying the contour inflection method due to the subjectivity of
352 deciding where the shape of the contour changes (Bate, 2008; Leonard and Fountain, 2003).

353

354 **Basal shear stress**

355 Glacier ice can flow via internal deformation, basal sliding and subsole deformation
356 (Piotrowski and Tulaczyk, 1999). The relative contribution of these flow types to the overall
357 behaviour of a glacier is determined by the pressure exerted by the ice on the bed, i.e. the
358 basal shear stress. Basal shear stress depends on ice thickness and ice surface slope, the
359 resistance of the glacier boundaries and ice viscosity:

$$360 \quad \tau_b = \rho g h \sin \alpha$$

361 where τ_b is basal shear stress, ρ is ice density (900 kg.m^{-3}), g is gravitational acceleration
362 (9.81 m.s^{-2}), h is mean ice thickness at the glacier's centreline (m), and α is the glacier surface
363 slope angle parallel to the ice flow direction; calculated in this study using the long profile 50
364 to 100 m either side of the ELA.

365

366 **Theoretical ice surface velocity**

367 The theoretical surface velocity at the glacier centreline due to ice deformation was
368 calculated by:

$$369 \quad U_s = \left(\frac{2 A \tau_b^n h}{n+1} \right) 31536000$$

370 where A is an ice-softness parameter of 5.3×10^{-15} , n is a constant (usually = 3, according to
371 Glen's Flow Law, h is ice thickness (m), and 31,536,000 is the number of seconds per year
372 (Kerschenner et al., 1999; Carr and Coleman, 2007). Theoretical velocity will differ from
373 actual velocity due to variation in glacier depth. Furthermore, this equation assumes that the

374 basal shear stress is driving movement in a direction parallel to the bed only (Benn and
375 Evans, 2010).

376

377 **Basal sliding and subsole deformation**

378 The likelihood of basal sliding or of subsole deformation can be determined by considering if
379 the reconstructed ice thickness was sufficient to melt the basal ice; i.e. if the bed of the
380 glacier was temperate, at pressure melting point (Golledge, 2012). At the pressure melting
381 point a film of meltwater between the ice and the bed surface reduces ice-bed friction and
382 encourages sliding. Additionally, this pressure and sliding could warm any basal sediments
383 and lead to flow due to deformation. Whether ice thickness at the ELA (h) is thick enough to
384 cause basal sliding (Weertman, 1961) can be calculated by:

$$385 \quad h \geq \left(K \frac{\Delta T}{Q_g + Q_s} \right) / 100$$

386 where K is the thermal conductivity of ice ($1.7 \times 10^5 \text{ cal.cm}^{-1}.\text{yr}^{-1}.\text{°C}^{-1}$), ΔT is the temperature
387 difference between the melting point of ice and the mean annual temperature of upper surface
388 of the glacier (°C), Q_g is the geothermal heat flux ($47.3 \text{ cal.cm}^{-2}.\text{yr}^{-1}$) and Q_s is the heat of
389 sliding friction (assumed to be 0).

390

391 **Theoretical steady state geometry**

392 An assessment of the degree to which the Ödenwinkelkees was out of equilibrium at each
393 time step was made firstly by comparing the geometrically-derived ice surface with that
394 suggested by a simple one-dimensional (1D) model applied along a centreline profile of the
395 glacier. The model was that presented by Benn and Hulton (2010), which assumes a steady
396 state ‘perfectly plastic’ ice rheology, where irrecoverable strain only occurs when the basal
397 shear stress equals a specified yield stress. We used a valley-wide yield stress of 130 kPa, as
398 suggested by Hoelzle et al., 2007 (from Haeberli and Hoelzle, 1995) as representative of
399 European Alps glaciers. Note that we did not tune the model in any way; e.g. to best fit the
400 height of lateral moraines; we wanted to consider the departure of the geometrically-
401 reconstructed ice surface to that of a theoretical steady state. Secondly, we analysed the
402 volume (V) - area (A) relationship given by $V = c.A^\gamma$ where $c = 0.027$ and $\gamma = 1.458$ for
403 steady state conditions (Adhikari and Marshall, 2012).

404

405 **Results: Changing geometry and behaviour of the Ödenwinkelkees**

406 Glacier terminus retreat, glacier length reductions and glacier ice surface lowering and ice
407 thickness reductions are depicted together in **Figure 5**. The Ödenwinkelkees terminus
408 position has retreated by ~ 1400m during the 163 years of the study (1850 – 2013), and is
409 now just 70 % of its 1850 length (~ 4600 m) (**Fig. 4**). A linear best-fit line represents the
410 change in absolute glacier length with $r^2 = 0.97$. The rate of change in the terminus position
411 reduced from -10 m.yr^{-1} between 1850 and 1890 to -5 m.yr^{-1} between 1890 and 1930, and
412 then increased to -25 m.yr^{-1} by 1980. Since 1980 the rate of change in the terminus position
413 has decreased from -25 m.yr^{-1} to $< -5 \text{ m.yr}^{-1}$.

414

415 The change in absolute glacier area (**Fig. 4**) has decreased by 40 % between 1850 to 2013 and
416 can be represented with a linear best-fit line with $r^2 = 0.98$. The rate of change of glacier area
417 was $\sim -0.01 \text{ km}^2.\text{yr}^{-1}$ between 1850 to 1970, but between 1970 to 1985 was positive (i.e.
418 enlarging) slightly. Between 1985 and 2013 the rate of change in glacier area has decreased
419 from $-0.01 \text{ km}^2.\text{yr}^{-1}$ to $0 \text{ km}^2.\text{yr}^{-1}$ (**Fig. 6**).

420

421 Mean ice thickness has reduced by 62 m and maximum ice thickness has reduced by 125 m
422 between 1850 and 2008; i.e. by 60 % and 43 % respectively of the reconstructed 1850 Ice
423 thickness. The rate of change in ice thickness between 1850 to 1977 varied between -0.5
424 m.yr^{-1} to 0.2 m.yr^{-1} ; i.e. a transition from losses in ice surface elevation to a period of time of
425 slight gain in ice surface elevation (**Fig. 6**). Ice thickness also increased at $\sim 0.5 \text{ m.yr}^{-1}$
426 between 1985 and 1992. There were prominent periods of ice surface lowering between 1977
427 and 1985 and between 1992 and 1998 at -0.25 m.yr^{-1} and -0.32 m.yr^{-1} , respectively (**Fig. 6**).

428

429 Glacier volume in 2008 was just 25 % of that reconstructed for the year 1850. The change in
430 absolute glacier volume through time can be represented by a linear best-fit line with $r^2 =$
431 0.94 (**Fig. 6**). The rate of change of volume has generally decreased from $-0.0025 \text{ km}^3.\text{yr}^{-1}$
432 between 1850 and 1890 to $-0.001 \text{ km}^3.\text{yr}^{-1}$ between 1998 and 2008. However, there was faster
433 rates of volume change both negative ($\sim -0.006 \text{ km}^3.\text{yr}^{-1}$) between 1977 and 1985 and
434 between 1992 and 1998, and positive ($\sim 0.001 \text{ km}^3.\text{yr}^{-1}$) between 1988 and 1992 (**Fig. 6**).

435

436 There is a large variation between the five different methods of calculating ELA, with an
437 average standard deviation of 63 m (**Fig. 6**). The AABR, AAR and Hmed methods
438 consistently overestimated the mean, whilst the THAR and the contour inflection methods
439 were consistently underestimating the mean. The glacier ELA, as reconstructed using the

440 mean of the five different map-based or geometric methods, increased by 90 m between 1850
441 and 2008, and can be represented by a linear best-fit line with $r^2 = 0.94$ (**Fig. 6**). The rate of
442 change of the ELA progressively increased between 1850 and 1950 (**Fig. 6**). However, the
443 times around 1985 and 1998 saw a drop in ELA elevation (**Fig. 6**). The application of
444 Weertman's (1961) equation suggests that ice thickness at the ELA has been consistently
445 thick enough to cause basal sliding, i.e. the glacier has had a temperate bed at all times since
446 1850 to the present day.

447
448 Basal shear stress, as calculated using the mean ice thickness on the centre line and the ice
449 surface gradient at this point, generally decreased from 260 kPa to 200 kPa between 1850 and
450 1992, as the glacier thinned (**Fig. 6**). However, in 1998 the mean basal shear stress had
451 dropped to 192 kPa and in 2008 to just 112 kPa, due to a reduction in ice surface gradient.
452 This rapid reduction in mean bed shear stress since the 1990s is interesting because Dreidger
453 and Kennard (1986) noted that glaciers in the Cascades apparently reached a thickness
454 sufficient to obtain a critical shear stress of 1 bar; i.e. 100 kPa. The rate of change of basal
455 shear stress was very slight between 1850 and 1977 but since 1988 has progressively and
456 rapidly decreased (**Fig. 6**).

457
458 Glacier velocity, as reconstructed using the mean ice thickness on the centre line and the ice
459 surface gradient at this point, and hence the mean basal shear stress, has decreased from 230
460 m.yr^{-1} to 10 m.yr^{-1} between 1850 and 2008 (**Fig. 6**). However, two distinct periods of
461 reductions in ice velocity are apparent; one between 1850 to 1932 and the other from 1969 to
462 2013 (**Fig. 6**).

463
464 The spatial pattern of ice elevation changes between successive reconstructions is represented
465 in **Figure 7**. The time periods 1950 to 1890, 1890 to 1929, 1929 to 1931, 1931 to 1969, 1969
466 to 1977 and 1998 to 2008 all exhibit some increase in ice surface elevation at higher altitudes,
467 and some ice surface lowering at lower altitudes (**Fig. 7**). Thereafter, the pattern of surface
468 elevation changes becomes more complex. The maps for the time periods 1977 to 1985 and
469 1992 to 1998 evidence surface lowering across virtually the entire glacier (**Fig. 7**). The maps
470 for the time periods 1985 to 1988 and 1988 to 1992 suggest ice surface elevation increases in
471 the easterly sections of the glacier and in the lower and central parts of the glacier,
472 respectively, but ice surface lowering at the higher altitude parts of the glacier (**Fig. 7**).
473 Between 2008 and 2013 the lower part of the glacier lost elevation. Asymmetric surface

474 elevation changes become clearer in more recent time periods; especially 1969 to 1977 and
475 1985 to 1988, where there is an east-west contrast in ice surface elevation changes (Fig. 7).

476
477 Comparison of the geometric profiles to that predicted by a theoretical steady state model is
478 only depicted in Figure 5 for selected time periods for clarity. A discrepancy between the
479 geometric profiles and the model-predicted profiles suggests that the Ödenwinkelkees has not
480 been in a steady state condition at any time. Figure 5 arguably suggests a progression
481 towards more equilibrium conditions with time towards the present day; one can compare the
482 geometric-model difference for 2008 and 1977 difference, which are both slight, with the
483 geometric-model difference of earlier time periods. The most obvious geometric-model
484 differences were in the glacier snout region, where the model consistently suggests higher
485 surface elevations than measured. The geometric and model surface elevation profiles tend to
486 converge towards the mid-reaches of the glacier. However, there was poor agreement
487 between the geometric and model centreline ice surface profiles in the upper steep head
488 region of the glacier, but Benn and Hulton (2010) acknowledge that the model does not do
489 well in steep headwall areas. Changing glacier 3D geometry is summarised in a series of
490 screenshots and a long profile graph in the supplementary information.

491
492 Analysis of the volume-area relationship for the Ödenwinkelkees at each time step (Fig. 8)
493 shows that the value of the exponent γ increased up until the 1970, suggesting a progressively
494 greater disequilibrium, and then a rapid decrease. The value of the exponent γ is now very
495 close to 1.458; that suggested by Adhakari and Marshall (2012) as representing steady state
496 conditions.

497

498 Discussion

499 This study highlights that the choice of geometric dimension(s) of glaciers that are considered
500 has a very big influence on the patterns, amounts and rates determined. Firstly, the decline in
501 glacier length in 2013 was 30 % of the 1850 length, the 2013 surface area was 61 % of the
502 1850 surface area, the maximum and mean thickness in 2008 was 50 % and 30 %, respectively
503 of those thicknesses in 1850, and the 2008 volume was only 24 % of the 1850
504 volume (Fig. 6a). Secondly, we found (small) increases in glacier volume that were not
505 reflected in area or length changes, which is an attribute of glacier adjustments to climate
506 recognised by Adhikari and Marshall (2012) with their volume-area analyses. Thirdly, whilst
507 the 1D, 2D and 3D measurements of absolute length, area and volume, respectively, all have

508 linear relationships with time (**Fig. 6a**), the effect of increasing complexity is best manifest in
509 the equation of these lines being used to predict when the glacier will cease to exist; the
510 length regression equation predicts no ice in the year 2354, that of area predicts no ice in the
511 year 2228 and that of volume predicts no ice in the year 2040. We therefore support the
512 widespread view that glacier length studies will only give an indication of glacier responses
513 to climate, whereas studies that include thickness and volume calculations provide much
514 more detailed and accurate knowledge of glacier dynamics processes (Bishop et al, 2004;
515 Dyurgerov and Meier, 2005; Kääb et al, 2002; Zemp, 2006).

516
517 Evidence of small re-advances in the 1890s, 1920s and early 1980s were expected with
518 consideration of the work by Knoll et al (2009). However, increases in ice mass were only
519 suggested by the data in this study for area and volume in 1985 (**Fig. 6**) and also for thickness
520 in the mid 1970s and mid 1980s. This lack of detection of an advance between 1850 to 1929
521 is due to the interval of measurements, which is not fine enough to capture evidence of re-
522 advance (Hoelzle et al, 2007). The positive ice thickness change in the mid-1970s is
523 unexpected but because: (i) the magnitude of the change is not outside of our level of
524 uncertainty, and (ii) this time period is outside of the studies of glacier inventories and thus of
525 most other alpine glacier geometry change studies.

526
527 Previous regional studies by Abermann (2011), Kääb et al. (2002), Bishop et al. (2004) and
528 Zemp (2006), for example have shown accelerating loss of ice volume; 48 % between 1850
529 and 1975 ($0.5 \% a^{-1}$), 25 % between 1975 and 2000 ($1 \% a^{-1}$), and 10 to 15 % between 2000
530 and 2005 ($3 \% a^{-1}$). The results of this study are in broad agreement for the same time
531 periods; 48 % between 1850 and 1975 ($0.5 \% a^{-1}$), 45 % between 1975 and 2000 ($1.8 \% a^{-1}$)
532 and 10 % between 2000 and 2005 ($2 \% a^{-1}$) but this study has many more intervals that can be
533 considered. With some caution because of our 20 m ice thickness uncertainty, the overall
534 volume changes calculated in this study for the period 1975 and 2000 are notable for being
535 twice the volume loss of ice reported in regionally-averaged studies.

536
537 The surface lowering calculated by this study for the Ödenwinkelkees ($0.4 m.a^{-1}$) is less than
538 half that reported to be the average across Austria, which was $1 m.a^{-1}$ (Fisher, 2009;
539 Lambrecht and Kuhn, 2007). This discrepancy is not likely to be due to the glacier size,
540 because Abermann et al.'s (2009) study of 81 different glaciers within the Otztal Alps in
541 Austria, suggested that glaciers of a similar size to the Ödenwinkelkees (1 to $5 km^2$) had an

542 average thickness of approximately 60 m (from the periods 1969 to 2007) and this fits well
543 with the thickness seen at the Ödenwinkelkees; where mean ice thickness reduced from 80 m
544 to 42 m over the same time period. Therefore the unexpectedly slow surface lowering is
545 probably due to more localised factors, namely supraglacial debris cover (**Fig. 2**) and
546 topography. The datasets used in this study do not include information of the spatial coverage
547 of supraglacial debris. However, qualitatively we consider that supraglacial debris cover
548 extent has increased as a proportion of the glacier surface between 1920 and the present day,
549 as based on our examination of historical postcards and paintings and photographs within the
550 Rudolfshuette.

551
552 Topographic effects are evidenced by asymmetric (east-west) thinning rates as depicted in
553 **Fig. 2**. Topography at the Ödenwinkelkees probably determines enhanced mass input from
554 lee side wind-redistributed snow deposition and from avalanching, and reduced mass loss due
555 to solar shading (**Fig. 2**). These topographic factors could have become more important as an
556 increasing proportion of the glacier has close proximity to steep surrounding headwalls (**Fig.**
557 **2**). These topographic factors could also explain why the ELA has risen by 67 m (**Fig. 6**)
558 rather than by 150 m as would be expected by a 1 °C air temperature rise that has been
559 observed across the Austrian Alps (e.g. Paul et al., 2007b), notwithstanding the fact that an
560 ELA value is theoretical and assumes equilibrium; a condition which is clearly not met.
561 Indeed recognition of a departure by the Ödenwinkelkees from modelled equilibrium
562 conditions (**Fig. 5**) is unsurprising, except for the LIA time period perhaps. However, it must
563 be remembered that in the absence of mapped outlines or surface contours for 1850 and 1890,
564 glacier surface profiles at those time periods were reconstructed using the position and
565 elevation of lateral moraines. Thus the difference between the 1850 and 1890 geometric and
566 modelled centreline surface profiles could provoke suggestions on the timing of lateral
567 moraine emplacement; at maximum ice extent or during ice thinning. **Figure 5** also evidences
568 spatiotemporally complex surface elevation (and hence mass) evolution. For example,
569 ablation area gains in 1969 to 1977 and between 1988 and 1992 are unrelated to regional
570 climate (warming) and thus could be indicative of a kinematic wave of mass moving down
571 glacier; mass that was derived from precipitation, wind re-distributed snow or avalanching,
572 for example.

573
574 Predictions of future relationships between length, area and volume with time, which
575 historically have been linear (**Fig. 6**) could be complicated by two factors. Firstly, the

576 estimated glacier bed surface indicates a number of undulations along its long profile, and
577 these are very likely real because their inflexions line up with pronounced topographic ridges
578 on either side of the glacier. These overdeepenings are likely sites for accumulation of
579 meltwater, which with diminishing overburden pressure as the ice thins will promote ice melt
580 and ice mass loss via calving and enhanced glacier terminus retreat (Benn et al., 2007; Kääb
581 and Haeberli, 2001; Linsbauer et al, 2012; Carrivick and Tweed, 2013).

582
583 Secondly, the present ELA at 2560 m a.s.l. coincides with the elevation of a very steep bed
584 surface and very thin ice; indeed there is bedrock protruding through the glacier ice surface at
585 this point (**Fig. 2b**); in other words the accumulation area is becoming physically separated or
586 decoupled from the ablation area. If this decoupling proceeds, then ice flow may reduce
587 dramatically or indeed stop altogether, leading to glacier stagnation in the lower part (Small,
588 1995; Linsbauer et al, 2012). The lower part of the glacier would continue to melt, albeit
589 slowly due to the supraglacial debris cover. The Ödenwinkelkees ice thickness trends support
590 this stagnation theory where continued reductions in thickness and surface slope have led to
591 basal stresses being reduced, most rapidly since the 1990s and towards the critical bed shear
592 stress limit of 1 bar (100 kPa) suggested by Dreidger and Kennard (1986). Between 1998 and
593 2008, basal shear stress dropped by 43 % and the associated maximum velocity (at the ELA)
594 by 82 % from 386 m a⁻¹ to 68 m a⁻¹ (c.f. Vacco et al, 2010).

595
596 Thirdly, the linear relationships between length, area and volume with time, could be
597 disrupted by the glacier apparently approaching a steady state condition, as suggested by the
598 V-A analysis (**Fig. 8**) and the progressive decline in the difference between a 1D steady state
599 model and our measured surface profiles (**Fig. 5**). Overall, the suggestion of increasing rate
600 of change in mountain glacier ice mass loss with time by Haeberli et al (2003), Zemp et al
601 (2007) and Abermann (2011) is far less pronounced in the results of this study. In fact this
602 study demonstrates decreased rates of change in glacier geometry; length, area and volume,
603 and glaciological parameters; bed shear stress and surface velocity, since 1980s to the
604 present.

605

606 **Conclusions and indications of future glacier response**

607 This study emphasises spatial heterogeneity and complexity in glacier responses to climate. It
608 contributes to bridging a gap between glacier inventories that have a high spatial but
609 comparably low temporal resolution, and length and mass balance records that have low

610 spatial but high temporal resolution. It quantifies absolute amounts, rates and trends of
611 changes in the 3D geometry of the Ödenwinkelkees glacier, central Austria, over thirteen
612 time periods spanning from 1850 to 2013.

613

614 The Ödenwinkelkees terminus position retreated by ~ 1400 m since the Little Ice Age; the
615 last Holocene maximum, and in 2013 was just 70 % of its former length. Glacier area
616 decreased by 40 % between 1850 and 2013 and glacier volume in 2008 was just 25 % of that
617 reconstructed for the year 1850. Regression equations of glacier length with time, area with
618 time and volume with time have r^2 values of > 0.94 , permitting prediction of no ice in the
619 year 2354 if using length, no ice in the year 2228 if using area, and no ice in the year 2040 if
620 using volume.

621

622 Volume-area scaling analyses and discrepancy between our reconstructed geometric profiles
623 and those suggested by a ‘perfect-plasticity’ model, both suggest that the Ödenwinkelkees
624 has not been in a steady state condition at any time in the last 160 years, but there has
625 arguably been evolution of the Ödenwinkelkees towards ‘equilibrium conditions’ with time
626 towards the present day. As another line of enquiry to see if the glacier was ‘stabilising’, we
627 had wished to compare the ‘climatic’ ELA; that suggested by lapse rates, with the
628 ‘geometric’ ELA; that suggested by measured glacier hypsometry, but the regional and local
629 weather data that we were able to obtain proved unsuitable in temporal coverage. Further
630 investigation of this idea of ‘glacier stabilisation’ could be made with hypsographic
631 modelling (c.f. Paul et al., 2007c).

632

633 We found a tendency for greater asymmetry in rates of change of reconstructed surface
634 elevation with more recent time periods, and we infer that this sheds light on processes that
635 may become more important for the state of the Ödenwinkelkees and other small mountain
636 glaciers in the future; namely mass inputs from avalanching and wind-blown snow, for
637 example, and topographic shading. We suggest that future geometric changes of the
638 Ödenwinkelkees and other small mountain glaciers will be controlled by ice thickness
639 thinning and ice surface slope reductions both together acting to reduce ice velocity. Together
640 with developing supraglacial debris cover and separation of the accumulation area from the
641 ablation area due to thinning over a bedrock ridge, conditions close to stagnation will ensue.
642 With the above conditions small mountain glaciers could become less sensitive to climate and
643 have longer response times.

644
645
646
647
648
649
650
651
652
653
654
655
656
657
658
659
660
661
662
663
664
665
666
667
668
669
670
671
672
673
674
675
676
677

There is no reason to suppose that the Ödenwinkelkees is unrepresentative of very many small mountain glaciers and the approach used in this study is directly applicable to other mountain glaciers, so the findings of this study should stimulate similar work at other sites and comparisons. The information on volume changes is effectively net balance (Paterson, 1994, p. 29), and so provides a good opportunity to quantify and compare glacier changes locally, regionally (c.f. Bauder et al., 2007) and even globally. Where there is confidence in 3D reconstructions, future studies could calculate ice-flux through selected cross-sections and balance gradients along the glacier tongue (Kerschner et al., 1999). Carr and Coleman (2007) more than adequately demonstrate the potential of gaining glaciologically meaningful information from geometric reconstructions. Where future studies encounter unknown bed topography, which is very common, it should be possible to use the trends within thickness and area parameters as methods of modelling ice thickness (Linsbauer et al., 2012; Raper and Braithwaite, 2009); the Ödenwinkelkees data of this study supports these models, for example, mean ice thickness accounts for 30 % of maximum ice thickness (with an error of 0.04 %) and there is a strong correlation between mean ice thickness increase with area, with a log scale trend (Linsbauer et al., 2012). Future work should quantify the effect of bed overdeepenings on ice dynamics, of supraglacial debris cover on the surface energy balance, and of local topographically-driven factors; namely wind-redistributed snow deposition, avalanching and solar shading, on mass balance.

Acknowledgements

Michael Kuhn is thanked for provision of the digital 1969 and 1998 datasets. Daniel Carrivick helped to collect the GPR data in 2010. Duncan Quincey is thanked for his comments on this work in progress. Andy Evans are thanked for their contributions in the field and discussions.

678 **References**

- 679 Abermann, J., Lambrecht, A., Fischer, A., and Kuhn, M., 2009. Quantifying changes and trends in glacier area
680 and volume in the Austrian Ötztal Alps (1969–1997–2006). *The Cryosphere Discussions*, 3, 415-441.
681
- 682 Adhikari, S., and Marshall, S. J., 2012. Glacier volume-area relation for high-order mechanics and transient
683 glacier states. *Geophysical Research Letters*, 39, L16505.
684
- 685 Austrian Alpine Club, 1969. Map of the Grossglockner region, 1:25,000. Austrian Alpine Club.
686
- 687 Austrian Alpine Club, 1985. Map of the Grossglockner region, 1:25,000. Austrian Alpine Club.
688
- 689 Bahr, D. B., Meier, M. F., and Peckham, S. D., 1997. The physical basis of glacier volume-area scaling. *Journal*
690 *of Geophysical Research: Solid Earth*, 102, 20355-20362.
691
- 692 Bahr, D. B., and Radić, V., 2012. Significant contribution to total mass from very small glaciers. *The*
693 *Cryosphere*, 6, 763-770.
694
- 695 Bate, S., 2008. A Reconstruction of Equilibrium Line Altitudes of the Little Ice Age Glaciers in Linnédalen,
696 Western Spitsbergen, Svalbard. MSc, University Centre in Svalbard
697
- 698 Bauder, A., Funk, M., and Huss, M., 2007. Ice-volume changes of selected glaciers in the Swiss Alps since the
699 end of the 19th century. *Annals of Glaciology*, 46, 145-149.
700
- 701 Benn, D. I., and Hulton, N. R., 2010. An Excel spreadsheet program for reconstructing the surface profile of
702 former mountain glaciers and ice caps. *Computers & Geosciences*, 36, 605-610.
703
- 704 Benn, D.I., and Lehmkuhl, F., 2000. Mass balance and equilibrium-line altitudes of glaciers in high mountain
705 environments. *Quaternary International*, 65-66, 15-29.
706
- 707 Binder, D., Brückl, E., Roch, K. H., Behm, M., Schöner, W., and Hynek, B., 2009. Determination of total ice
708 volume and ice-thickness distribution of two glaciers in the Hohe Tauern region, Eastern Alps, from GPR data.
709 *Annals of Glaciology*, 50, 71-79.
710
- 711 Bishop, M.P., Haerberli, W., Käab, A., Paul, F., Hall, D. K., Kargel, J. S., Molnia, B. F., Trabant, D. C.,
712 Wessels, R., Olsenholler, J. A., Shroder, J. F., Barry, R. G., Raup, B. H., Bush, A. B. G., Copland, L., Dwyer J.
713 L. and Fountain, A. G., 2004. Global land ice measurements from space (GLIMS): Remote sensing and GIS
714 investigations of the Earth's cryosphere. *Geocarto International*. 19, 57-84.
715
- 716 Carr, S., and Coleman, C., 2007. An improved technique for the reconstruction of former glacier mass-balance
717 and dynamics. *Geomorphology*, 92, 76-90.
718
- 719 Carrivick, J. L. and Brewer, T. R., 2004. Improving local estimations and regional trends of glacier equilibrium
720 line altitudes. *Geografiska Annaler*, 86A, 67-79
721
- 722 Carrivick, J. L., and Rushmer, E. L., 2009. Inter- and Intra-catchment variability in proglacial geomorphology:
723 An example from Franz Josef Glacier and Fox Glacier, South Westland, New Zealand. *Arctic, Antarctic and*
724 *Alpine Research*, 41, 18-36.
725
- 726 Carrivick, J. L., and Chase, S. E., 2011. Spatial and temporal variability in the net mass balance of glaciers in
727 the Southern Alps, New Zealand. *New Zealand Journal of Geography and Geophysics*, 54, 415-429.
728
- 729 Carrivick, J.L., Tweed, F.S., 2013. Proglacial lakes: character, behaviour and geological importance.
730 *Quaternary Science Reviews*, 78, 34–52.
731
- 732 Carrivick, J. L., Davies, B. J., Glasser, N. F., Nyvlt, D., and Hambrey, M. J., 2012. Late-Holocene changes in
733 character and behaviour of land-terminating glaciers on James Ross Island, Antarctica. *Journal of Glaciology*,
734 58, 1476-1490.
735

- 736 Carrivick, J. L., Geilhausen, M., Warburton, J., Dickson, N. E., Carver, S.J., Evans, A. E., Brown, L. E., 2013.
737 Contemporary geomorphological activity throughout the proglacial area of an alpine catchment.
738 *Geomorphology*, 188, 83-95
739
- 740 Chinn, T. J. H., 1995. Glacier fluctuations in the Southern Alps of New Zealand determined from snowline
741 elevations. *Arctic and Alpine Research*, 27, 187-198.
742
- 743 Cornelius and Clar, 1929. Geologische karte des Groglockergebietes. Aufgenommen im Auftrage des
744 Deutschen u. Österreischen Alpenvereins.
745
- 746 Driedger, C. L., and Kennard, P.M., 1986. Glacier volume estimation on Cascade volcanoes: an analysis and
747 comparison with other methods. *Annals of Glaciology*, 8, 59-64.
748
- 749 Dyurgerov M. B., and Meier, M. F., 2005. *Glaciers and the changing Earth system: a 2004 snapshot* (Occasional
750 Paper 58, Institute of Arctic and Alpine Research, Univ. of Colorado, Boulder, Colorado).
751
- 752 Farinotti, D., Huss, M., Bauder, A., Funk, M., and Truffer, M., 2009. A method to estimate the ice volume and
753 ice-thickness distribution of alpine glaciers. *Journal of Glaciology*, 55, 422-430.
754
- 755 Federal Office of Metrology and Surveying, 1931. *Grosglockner*, 1:50000, Vienna: Federal Office of Metrology
756 and Surveying.
757
- 758 Gardent, M., Rabatel, A., Dedieu, J. P., and Deline, P., 2014. Multitemporal glacier inventory of the French
759 Alps from the late 1960s to the late 2000s. *Global and Planetary Change*. 120, 24–37.
760
- 761 Glasser, N. F., Harrison, S., Jansson, K. N., Anderson, K. and Cowley, A. 2011. Global sea-level contribution
762 from the Patagonian Icefields since the Little Ice Age maximum. *Nature Geoscience*, 4(5), 303-307.
763
- 764 Golledge, N. A., Mackintosh, A. N., Anderson, B. M., Buckley, K. M., Doughty, A. M., Barrell, D. J. A.,
765 Denton, G. H., Vandergoes, M. J., Andersen, B. G. and Schaefer, J. M., 2012. Last Glacial Maximum climate in
766 New Zealand inferred from a modelled Southern Alps icefield. *Quaternary Science Reviews*, 46, 30-45.
767
- 768 Gross, G., 1987: Der Flächenverlust der Gletscher in Österreich 1850–1920–1969. *Zeitschrift für*
769 *Gletscherkunde und Glazialgeologie*, 23, 131-141.
770
- 771 Haeberli, W., and Hölzle, M., 1995. Application of inventory data for estimating characteristics of and regional
772 climate-change effects on mountain glaciers: a pilot study with the European Alps. *Annals of Glaciology*, 21,
773 206-212.
774
- 775 Haeberli, W., Hoelzle, M., Paul, F., and Zemp, M., 2007. Integrated monitoring of mountain glaciers as key
776 indicators of global climate change: the European Alps. *Annals of Glaciology*, 46, 150-160.
777
- 778 Hall, D. K., Bayr, K. J., Schöner, W., Bindschadler, R. A., & Chien, J. Y. 2003. Consideration of the errors
779 inherent in mapping historical glacier positions in Austria from the ground and space (1893–2001). *Remote*
780 *Sensing of Environment*, 86(4), 566-577.
781
- 782 Harrison, W. D., Cox, L. H., Hock, R., March, R. S., and Petit, E. C., 2009. Implications for the dynamic health
783 of a glacier from comparison of conventional and reference-surface balances, *Annals of Glaciology*, 50, 25–30.
784
- 785 Harrison, S., Rowan, A.V., Glasser, N.F., Knight, J., Plummer, M.A. and Mills, S., 2014. Little Ice Age glaciers
786 in Britain: glacier-climate modeling in the Cairngorms. *The Holocene*, 24(2), 135-140.
787
- 788 Hoelzle, M., Haeberli, W., Dischl, M., and Peschke, W., 2003. Secular glacier mass balances derived from
789 cumulative glacier length changes. *Global and Planetary Change*, 36, 295-306.
790
- 791 Hoelzle, M., Chinn, T., Stumm, D., Paul, F., Zemp, M., and Haeberli, W., 2007. The application of glacier
792 inventory data for estimating past climate change effects on mountain glaciers: A comparison between the
793 European Alps and the Southern Alps of New Zealand. *Global and Planetary Change*, 56, 69-82.
794

- 795 Hormes, A., Beer, J., and Schlüchter, C., 2006. A geochronological approach to understanding the role of solar
796 activity on Holocene glacier length variability in the Swiss Alps. *Geografiska Annaler A*, 88, 281-294.
797
- 798 Huss, M., 2012. Extrapolating glacier mass balance to the mountain range scale: the European Alps 1900–2100.
799 *The Cryosphere Discussions*, 6, 1117-1156.
800
- 801 Humlum, O., 2002. Modelling late 20th-Century precipitation in Nordenskiöld Land, Svalbard, by geomorphic
802 means. *Norsk Geografisk Tidsskrift* 56, 96-103.
803
- 804 Hutchinson, M. F., 1989. A new procedure for gridding elevation and stream line data with automatic removal
805 of spurious pits. *Journal of Hydrology*, 106, 211-232.
806
- 807 Käab, A., Paul, F., Maisch, M., Hoelzle, M., and Haeblerli, W., 2002. The new remote-sensing-derived Swiss
808 glacier inventory: II. First results. *Annals of Glaciology*, 34, 362-366.
809
- 810 Kerschner, H., S.Ochs and C. Schlüchter. 1999. Paleoclimatic interpretation of the early late-glacial glacier in the
811 Gschnitz valley, Central Alps, Austria. *Annals of Glaciology*, 28, 135-140
812
- 813 Klok, E. J., and Oerlemans, J., 2004. Climate reconstructions derived from global glacier length records. *Arctic,*
814 *Antarctic, and Alpine Research*, 36, 575-583.
815
- 816 Knoll, C., Kerschner, H., Heller, A. and Rastner, P., 2009. A GIS-based Reconstruction of Little Ice Age Glacier
817 Maximum Extents for South Tyrol, Italy. *Transactions in GIS*. 13, 449-463.
818
- 819 Kuhn, M., Lambrecht, A., Abermann, J., Patzelt G., and Groß, G., 2009. Die österreichischen Gletscher 1998
820 und 1969, Flächen- und Volumenänderungen. Wien: Verlag der österreichischen Akademie der Wissenschaften.
821
- 822 Lambrecht, A., and Kuhn, M., 2007. Glacier changes in the Austrian Alps during the last three decades, derived
823 from the new Austrian glacier inventory. *Annals of Glaciology*, 46, 177-184.
824
- 825 Leonard, K.C., and Fountain, A.G., 2003. Map-based methods for estimating glacier equilibrium-line altitudes.
826 *Journal of Glaciology*, 49, 329-336.
827
- 828 Li, H., Ng, F., Li, Z., Qin, D., and Cheng, G., 2012. An extended “perfect-plasticity” method for estimating ice
829 thickness along the flow line of mountain glaciers. *Journal of Geophysical Research: Earth Surface*, 117(F1).
830
- 831 Linsbauer, A., Paul, F., and Haeblerli, W., 2012. Modeling glacier thickness distribution and bed topography
832 over entire mountain ranges with GlabTop: Application of a fast and robust approach. *Journal of Geophysical*
833 *Research*, 117(F3).
834
- 835 Mennis, J. L., and Fountain, A. G., 2001. A spatio-temporal GIS database for monitoring alpine glacier change.
836 *Photogrammetric engineering and remote sensing*, 67, 967-974.
837
- 838 Nesje, A., 1992. Topographical Effects on the Equilibrium-Line Altitude on Glaciers. *GeoJournal*, 27, 383-391.
839
- 840 Oerlemans, J., 2005. Extracting a climate signal from 169 glacier records. *Science*, 308, 675-677.
841
- 842 Osmaston, H., 2005. Estimates of glacier equilibrium line altitudes by the Area× Altitude, the Area× Altitude
843 Balance Ratio and the Area× Altitude Balance Index methods and their validation. *Quaternary International*,
844 138, 22-31.
845
- 846 Patzelt, G., 1980. The Austrian glacier inventory: status and first results. *IAHS Publication (Riederalp*
847 *Workshop 1978 – World Glacier Inventory)*, 126, 181-183.
848
- 849 Paul, F., 2002. Changes in glacier area in Tyrol, Austria, between 1969 and 1992 derived from Landsat 5
850 Thematic Mapper and Austrian Glacier Inventory data. *International Journal of Remote Sensing*, 23, 787-799.
851
- 852 Paul, F., 2010. The influence of changes in glacier extent and surface elevation on modeled mass balance. *The*
853 *Cryosphere Discussions*, 4, 737-766.
854

- 855 Paul, F., and Haeberli, W., 2008. Spatial variability of glacier elevation changes in the Swiss Alps obtained from
856 two digital elevation models. *Geophysical Research Letters*, 35, L21502.
857
- 858 Paul, F., Kääb, A., Haeberli, W., 2007a. Recent glacier changes in the Alps observed by satellite: Consequences
859 for future monitoring strategies. *Global and Planetary Change*, 56, 11-122.
860
- 861 Paul, F., Maisch, M., Rothenbühler, C., Hoelzle M., and Haeberli, W., 2007b. Calculation and visualisation of
862 future glacier extent in the Swiss Alps by means of hypsographic modelling. *Global and Planetary Change* 55,
863 343-357.
864
- 865 Paul, F., Maisch, M., Rothenbühler, C., Hoelzle, M., & Haeberli, W. (2007c). Calculation and visualisation of
866 future glacier extent in the Swiss Alps by means of hypsographic modelling. *Global and Planetary Change*,
867 55(4), 343-357.
868
- 869 Piotrowski, J., and Tulaczyk, S., 1999. Subglacial conditions under the last ice sheet in northwest Germany:
870 ice-bed separation and enhanced basal sliding? *Quaternary Science Reviews*, 18, 737-751.
871
- 872 Porter, S. C., 2001. Snowline Depression in the Tropics During the Last Glaciation'. *Quaternary Science*
873 *Reviews*, 20, 1067-1091.
874
- 875 Raper, S and Braithwaite, R., 2009. Glacier volume response time and its links to climate and topography based
876 on a conceptual model of glacier hypsometry. *The Cryosphere*, 3, 183-194.
877
- 878 Rippin, D. M., Carrivick, J. L., and Williams, C., 2011. Evidence towards a thermal lag in the response of small
879 Arctic glaciers to climate change. *Journal of Glaciology*, 57, 895-903.
880
- 881 Slupetzky, H., and Teufl, J., 1991. Ödenwinkelkees Gletschervorfeld 1:5000. Institut für kartographie und
882 reproduktionstechnik (IKR). Universität Salzburg und Oesterreichischer Alpenverein.
883
- 884 Steiner, L., 2011. Reconstruction of Glacier States from Geo-Referenced, Historical Postcards. Masters thesis.
885 Eidgenössische Technische Hochschule Zurich. 54 pages plus appendices.
886
- 887 Stocker-Waldhuber, M., Wiesenegger, H., Abermann, J., Hynek, B., and Fischer, A.; 2012. A new glacier
888 inventory of the province of Salzburg, Austria 2007/2009. *Zeitschrift für Gletscherkunde und Glazialgeologie*,
889 43, 121-128.
890
- 891 Vacco, D.A. R. Alley, D. Pollard and D. Reusch. 2010. Numerical modeling of valley glacier stagnation as a
892 paleoclimatic indicator *Quaternary Research*, 73, 403-409
893
- 894 Villa, F., De Amicis, M., and Maggi, V., 2007. GIS analysis of Rutor Glacier (Aosta Valley, Italy) volume and
895 terminus variations. *Geografia fisica e dinamica quaternaria*, 30, 87-95.
896
- 897 Vincent, C., Kappenberger, G., Valla, F., Bauder, A., Funk, M., and Le Meur, E., 2004. Ice ablation as evidence
898 of climate change in the Alps over the 20th century. *Journal of Geophysical Research: Atmospheres*, 109(D10).
899
- 900 Weertman, J., 1961. Stability of Ice-Age Ice Sheets. *Journal of Geophysical Research*, 66, 3783-3792.
901
- 902 ZAMG, 2014. Historical Instrumental Climatological Surface Time Series Of The Greater Alpine Region.
903 <http://www.zamg.ac.at/histalp/> last visited 28/11/14.
904
- 905 Zemp M., 2006. *Glaciers and climate change. Spatiotemporal analysis of glacier fluctuations in the European*
906 *Alps after 1850.* Zürich: Universität Zürich,
907
- 908 Zemp, M., Paul, F., Hoelzle, M., and Haeberli, W., 2008. *Glacier Fluctuations in the European Alps, 1850-2000.*
909 *Darkening Peaks: Glacier Retreat, Science, and Society*, 152 pp.
910
- 911 Zumbühl, H. J., Steiner, D., and Nussbaumer, S. U., 2008. 19th century glacier representations and fluctuations
912 in the central and western European Alps: An interdisciplinary approach. *Global and Planetary Change*, 60, 42-
913 57.

914 Decadal-scale changes of the Ödenwinkelkees, central Austria, suggest increasing control of
 915 topography and evolution towards steady state
 916 Jonathan L. Carrivick and Katie Berry
 917

Data type	Date of glacier extent	Source
Digitised outline of 1850 moraines. Thought to be the maximum extent during the Little Ice Age.	1850	Primary dataset, field geomorphological survey and digitised from catchment DEM from ALS data Carrivick et al. (2013). Moraine date from historical observations compiled by Slupetzky and Teufl (1991)
1:250,000 map of the Hohe Tauern Range	1880 - 88	Karte der Ost-Tiroler-Alpen, Tauern & Dolomiten (Karte der Ostalpen, Blatt V), Maßstab 1:250.000. Frankfurt, Ludwig Ravenstein Verlag (1889)
Digitised outline of 1890 extent from moraines.	1890	Primary dataset, field geomorphological survey and digitised from the catchment DEM (Carrivick et al, 2013). Moraine date from historical observations compiled by Slupetzky and Teufl (1991)
Austrian topographic map 1:25,000	1929 - 32	Federal Office of Metrology and Surveying (1931?)
Geological map of the Grossglockner region 1:25,000	1929(?)	Cornelius and Clar (1929)
Austrian Alpine Club map 1:25,000	1969	Austrian Alpine Club (1969)
Ice surface DEM from the Austrian Glacier Inventory.	1969	Gross (1987) and Patzelt (1980)
Austrian topographic map 1:25,000	1977	Unknown glacier extent date, therefore, the date was approximated using its position relative to other dated extents and supported by work by Kuhn et al (2009)
Orthophoto of the Ödenwinkelkees.	1979	Federal Office of Metrology and Surveying (1979)
Geological map of Austria 1:50,000 scale	1985	Höck and Pestal (1994)
Austrian Alpine Club map 1:25,000	1985 (B)	Austrian Alpine Club (1985)
Topographic map 1:50,000 scale	1988	Official Austrian topographic map (Federal Office of Metrology and Surveying, N.D). Glacier extent date unknown, therefore approximated using its position relative to other dated extents and supported by work by Kuhn et al. (2009) and Slupetzky and Teufl (1991)
Austrian topographic map 1:50,000 scale	1992	Federal Office of Metrology and Surveying (1992)
Ice surface DEM from the Austrian Glacier Inventory.	1998	Lambrecht and Kuhn (2007)
Catchment DEM	2008	Carrivick et al. (2013)
Ground Penetrating Radar data (ice thickness).	1998 2010	Span et al. (2005) Unpublished surveys made by Jonathan Carrivick, Christopher Williams and Daniel Carrivick in April 2010 and processed by David Rippin

918 **Table 1** Datasets used in this study to reconstruct Ödenwinkelkees geometry and discrete
 919 time increments.

920

921 Decadal-scale changes of the Ödenwinkelkees, central Austria, suggest increasing control of
 922 topography and evolution towards steady state
 923 Jonathan L. Carrivick and Katie Berry
 924

Source of error	Error acknowledgement and management
Original map production	Error exists within the original mapping of ~ 5% error; we have calculated difference between three 1985 datasets. This error is deemed acceptable for the purpose of this study. We note that this method is used throughout the literature (due to its simplicity) and effectiveness in capturing ice extent, thereby permitting further analysis (e.g. Mennis and Fountain, 2001; Kääh et al, 2002; Hoelzle et al, 2007; Lambrecht and Kuhn, 2007; Paul and Andreassen, 2009).
Original map scale	Unquantifiable uncertainty due to data used to construct the map and also the map scales (1:25,000 and 1:50,000), which introduce error through cartographic generalisation.
Interpreting 1850 and 1890 extents	The interpretation of the lateral moraines is in places obvious, and in others less so due to some degradation since deposition. Reconstruction of the accumulation area outline is much more difficult and largely subjective by examining any supposed trimlines.
Estimating 1850 and 1890 ice surface contours	There is no available evidence of the shape and position of the contour lines for the interpreted 1850 and 1890 extents. The elevation of the outline was taken from the catchment DEM. It was clear from more recent datasets that the ice surface contours were concave in the accumulation zone and convex in the ablation zone (c.f. Leonard and Fountain, 2003). Therefore, the general shape of the 1929 contours were used to estimate the ice surfaces but they were 'lifted' and 'extended across-valley' to intersect with the 1850 and 1890 outlines.
Positional error	Georeferencing positional errors were minimised by positioning all layers relative to the 2008 LiDAR data, i.e. to the best positioned layer multiple control points (c.f. Mennis and Fountain, 2001).
Glacier extent digitisation	The digitisation processes inherently causes cartographic generalisation, the level of detail captured depends on the person digitising and the amount of time available, as it is a very labour intensive process. The highest possible level of detail was aimed for, trying to take into account every small "finger". However, these fingers varied on the original maps, sometimes classed as part of the glacier, other times classed as disconnected. This could be reflective of the actual state of the glacier during certain times or it could be down to subjectivity of the map creator as to their classification (c.f. Mennis and Fountain, 2001).
Contour map digitisation	This incorporates errors from the original historical map and from the digitisation process. Leonard and Fountain (2003) suggest that contour error is typically half the contour interval, which in this case was 10 m. Where possible DEMs from remotely sensed data were used as the ice surface (for 1969, 1998 and 2008), which reduced this error.
Surface DEM creation	Interpolation between the 20 m interval contour lines varies depending on the method used (e.g. inverse distance weighting, spline, kriging etc.) but generally does not negatively affect the results, and is a good method of estimating previous ice surfaces (Mennis and Fountain, 2001).
ELA calculations	There has been wide discussion on the errors of the methods of ELA calculations (e.g. Benn and Lehmkuhl, 2000; Leonard and Fountain, 2003; Porter, 2001). Therefore, to avoid bias due to choosing one method, four methods were applied in this study (all appropriate to mountain glaciers) and the mean value was used for further calculations.

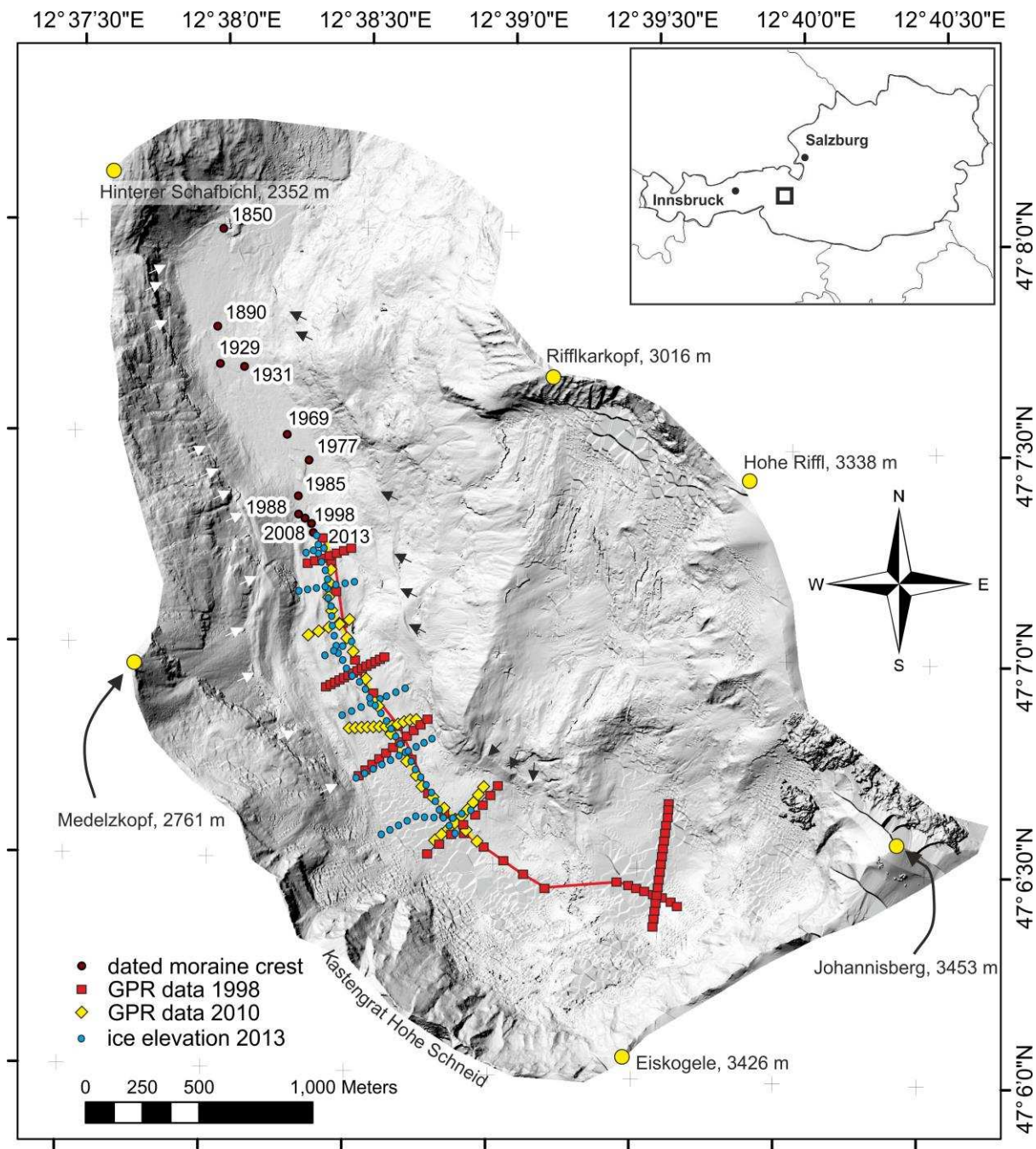
925
 926 **Table 2** Sources of error within the glacial reconstruction methodology and their
 927 management. These errors are to be expected when working with such old datasets (in
 928 addition to the modern datasets).

929
 930
 931

932 Decadal-scale changes of the Ödenwinkelkees, central Austria, suggest increasing control of
933 topography and evolution towards steady state

934 Jonathan L. Carrivick and Katie Berry

935



936

937 **Figure 1** Study location and detail of the Ödenwinkelkees and its catchment, central Austria.
938 The hillshaded elevation model (main image) is derived from airborne LiDAR (ALS) data
939 gridded at 1 m resolution. The terminal moraines of the 1850, 1890 and 1929 extents as dated
940 by Slupetzky and Teufl (1991) are visible in this terrain model, as are associated lateral
941 moraines and trimlines, the upper limit of which is indicated by the white and black arrows
942 on the west and east hillsides, respectively.

943 Decadal-scale changes of the Ödenwinkelkees, central Austria, suggest increasing control of
944 topography and evolution towards steady state

945 Jonathan L. Carrivick and Katie Berry

946



947

948

949

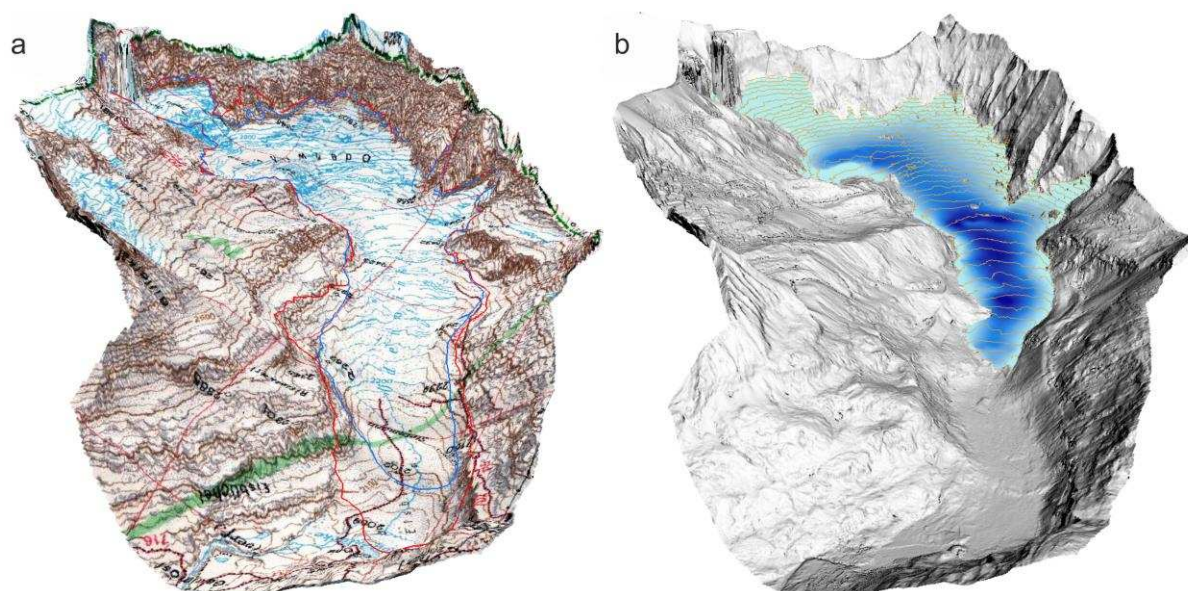
950

951 **Figure 2** Field photographs annotated with 1850 and 1890 glacier extents; white dashed lines
952 in part a, and separation of accumulation area via ice thinning over bedrock steps; black
953 arrows in parts a and b. Note east-west asymmetry in surface of glacier; perpendicular to
954 valley axis, in b. Part c depicts April 2010 GPR data collection using 50 Hz antennae
955 mounted on a manhailed sledge.

956 Decadal-scale changes of the Ödenwinkelkees, central Austria, suggest increasing control of
957 topography and evolution towards steady state

958 Jonathan L. Carrivick and Katie Berry

959



960

961

962

963 **Figure 3** Indication of some of the data sets used in this study; digitisation of glacier outlines
964 from historical maps (a) and from geomorphological evidence (b), coupled with ice thickness
965 (part b; blue shades) derived from ground penetrating radar surveys.

966

967

968

969

970

971

972

973

974

975

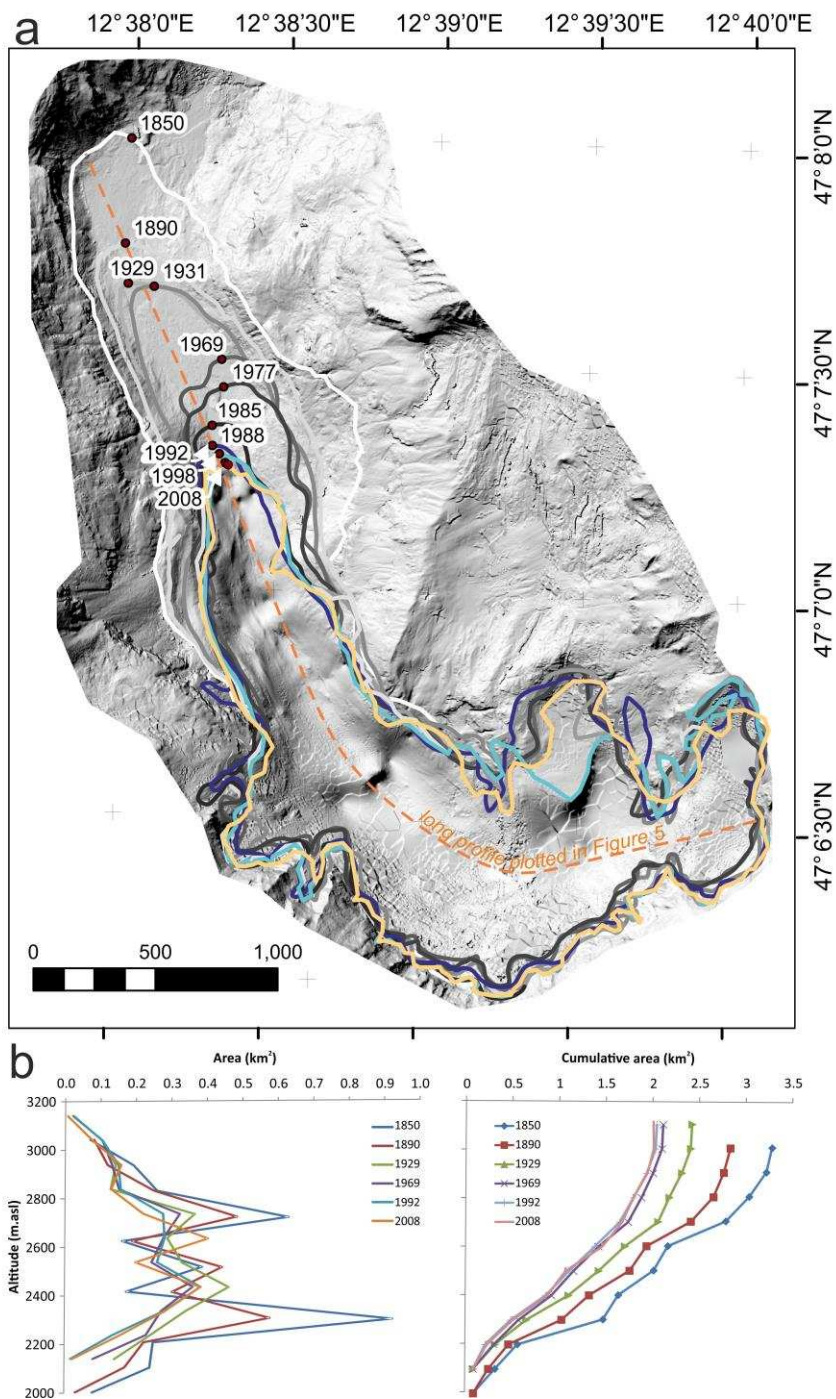
976

977

978

979 Decadal-scale changes of the Ödenwinkelkees, central Austria, suggest increasing control of
 980 topography and evolution towards steady state

981 Jonathan L. Carrivick and Katie Berry



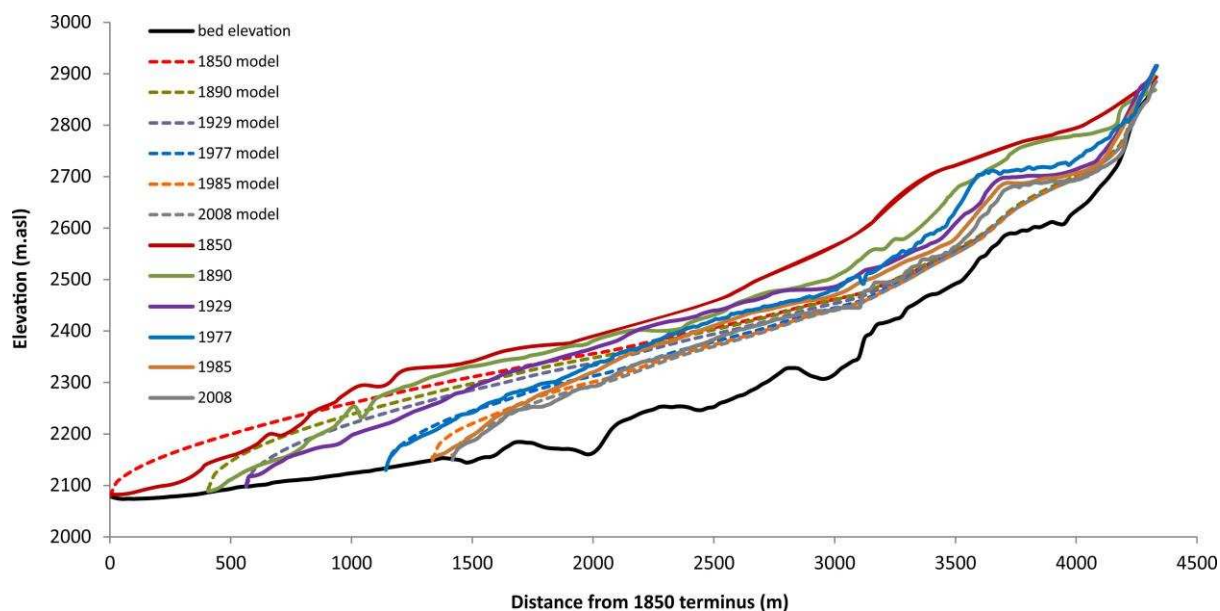
982
 983 **Figure 4** Reconstructed glacier outlines for 1850 and 1890, and mapped glacier outlines for
 984 1929 to 2008 (a). The hillshaded DEM in part A includes the estimated glacier bed, i.e. with
 985 the contemporary ice thickness removed. The centre line as mapped in part a is that used to
 986 define the long profiles in Figure 5. Reconstructed glacier hypsometry is depicted in part b.

987 Decadal-scale changes of the Ödenwinkelkees, central Austria, suggest increasing control of
988 topography and evolution towards steady state

989 Jonathan L. Carrivick and Katie Berry

990

991



992

993

994 **Figure 5** Reconstructed ice surface elevations along a centre-line long profile (solid lines)
995 compared with those modelled (dashed lines) using a steady-state ‘perfect-plasticity’ 1D
996 model.

997

998

999

1000

1001

1002

1003

1004

1005

1006

1007

1008

1009

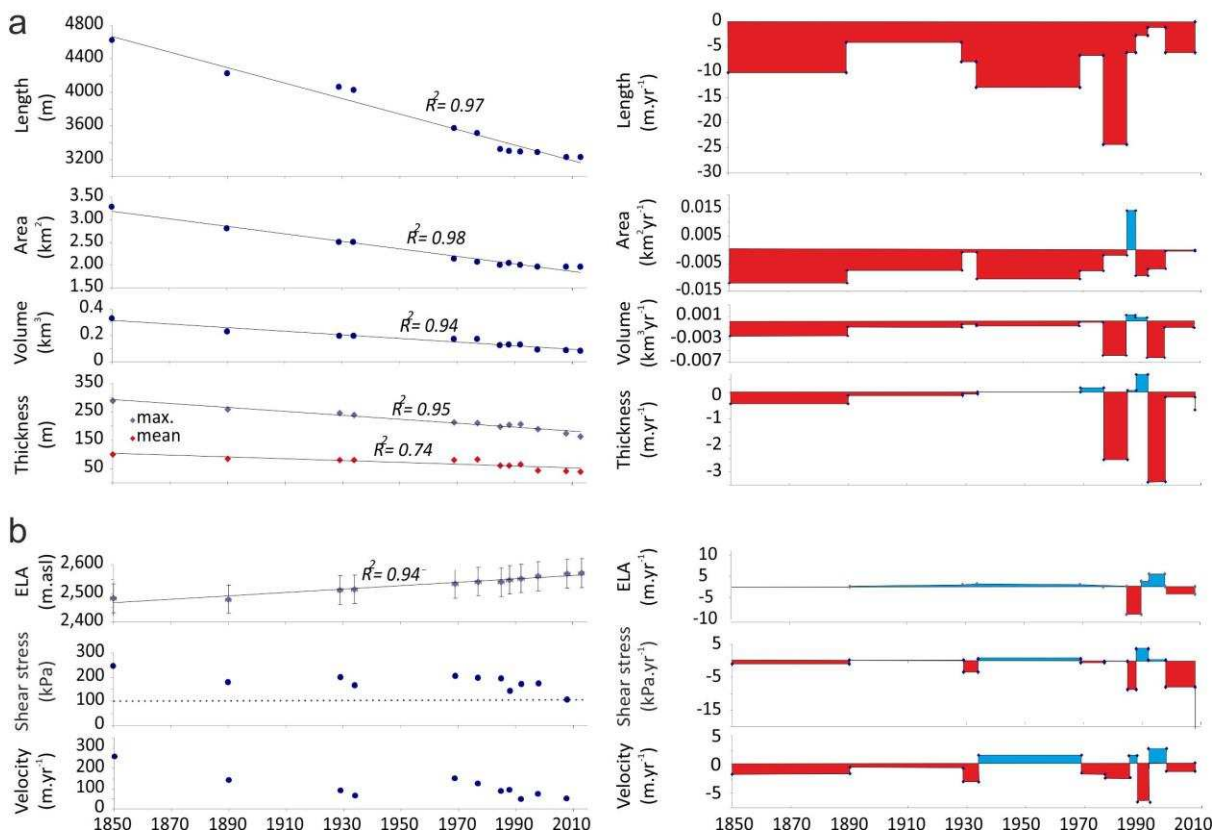
1010

1011 Decadal-scale changes of the Ödenwinkelkees, central Austria, suggest increasing control of
 1012 topography and evolution towards steady state

1013 Jonathan L. Carrivick and Katie Berry

1014

1015



1016

1017

1018

1019

1020

1021

1022 **Figure 6** Reconstructed absolute measures of glacier geometry; length, area, volume and
 1023 thickness (a), and glaciological properties; ELA, shear stress, velocity, both with
 1024 corresponding rates of change (b). The dashed line in the absolute bed shear stress panel is
 1025 the critical bed shear stress of 1 bar (100 kPa) suggested by Dreydger and Kennard (1986).

1026

1027

1028

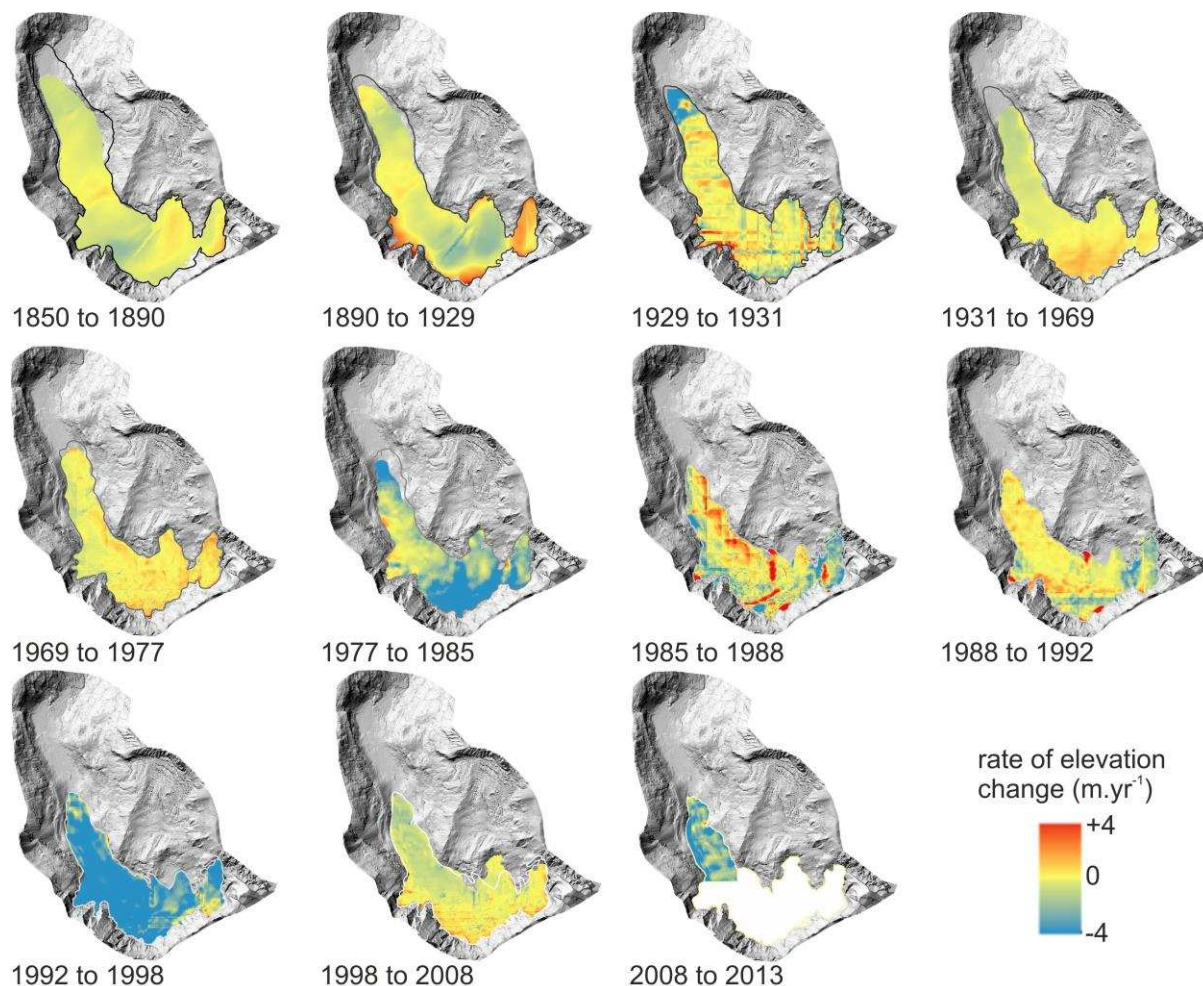
1029

1030 Decadal-scale changes of the Ödenwinkelkees, central Austria, suggest increasing control of
1031 topography and evolution towards steady state

1032 Jonathan L. Carrivick and Katie Berry

1033

1034



1035

1036

1037 **Figure 7** Spatiotemporal variability in the rate of elevation change of the Ödenwinkelkees.

1038

1039

1040

1041

1042

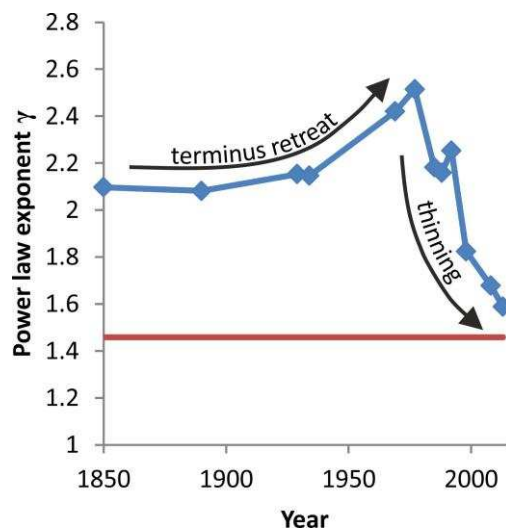
1043

1044

1045 Decadal-scale changes of the Ödenwinkelkees, central Austria, suggest increasing control of
1046 topography and evolution towards steady state

1047 Jonathan L. Carrivick and Katie Berry

1048



1049

1050

1051 **Figure 8** Suggestion of evolution of Ödenwinkelkees glacier geometry towards equilibrium
1052 as represented by Adhikari and Marshall's (2012) volume-area power law exponent γ . The
1053 red line with value 1.458 is that determined for mountain glaciers in steady state by Adhikari
1054 and Marshall (2012). Up until 1970 the dominant geometric change at Ödenwinkelkees was
1055 terminus retreat, whilst post-1970 geometric change was dominantly thinning.